Investigating the ARSIRI Model: An Extended SIR Model with Reinfection for Modelling Addiction-Related Phenomena

N. Susyanto (iD)

*Department of Mathematics, Universitas Gadjah Mada,
Yogyakarta, Indonesia*

E-mail: nanang_susyanto@ugm.ac.id
*Corresponding author

Abstract

This paper investigates the ARSIRI model, a modified SIR model that considers the possibility of reinfection from the recovered compartment to the infected compartment. This modification is motivated by representing an addiction-related phenomenon in which recovered individuals can become reinfected. The paper examines disease-free and endemic equilibrium points. The stability conditions of the equilibrium points are investigated using a reproductive number that cannot be computed using the regular next-generation matrix. The most important parameter in the model, namely the reinfection rate, is then analyzed from a bifurcation point of view. Finally, the ARSIRI model is applied to simulated data as well as real data related to alcohol addiction, demonstrating its superiority over the regular SIR model.

Keywords: ARSIRI model; equilibrium points; reproductive number; bifurcation analysis; alcohol addiction model.

1   Introduction

Mathematical modelling plays a vital role in addressing diverse real-world problems by providing critical insights and solutions. Researchers utilize mathematical principles to abstract complex phenomena into models, enabling effective analysis, prediction, and decision-making. In public health and epidemiology, as shown in [16, 7], modelling is employed to simulate disease spread, assess interventions, and inform policy formulation. Similarly, phenomena such as predator-prey interactions can also be effectively modeled mathematically [8]. In another application, mathematical models are used to elucidate how smoking behaviors propagate within a population [5]. Furthermore, mathematical approaches, such as those proposed in [15], contribute to advancements in classification methods. An additional intriguing application is the modelling of social dynamics, as highlighted in [4].

Among all the mentioned models, the Susceptible-Infected-Recovered (SIR) model is one of the most common. This model is a well-established compartmental model used to understand the spread of infectious diseases [6]. It divides a population into three compartments: susceptible (S), infected (I), and recovered (R). Zhang et al. [22] consider an SIR model for modelling disease spread constant infectious period. They provide conditions under which the disease dies out or becomes endemic, giving insight into the long-term behavior of the disease.
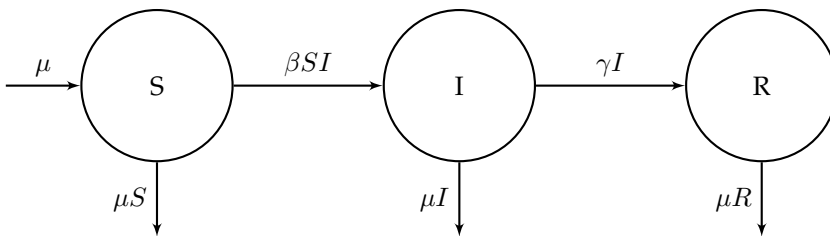

Figure 1: SIR Diagram Transfer

With β representing the infection rate and γ representing the recovery rate, and referring to the transfer diagram shown in Figure 1, SIR model is expressed as a system of differential equations:

$$
\begin{aligned}
\frac{dS(t)}{dt} &= \mu - \beta S(t)I(t) - \mu S(t), \; S(0) = S_0 \geq 0, \\
\frac{dI(t)}{dt} &= \beta S(t)I(t) - \mu I(t) - \gamma I(t), \; I(0) = I_0 \geq 0, \\
\frac{dR(t)}{dt} &= \gamma I(t) - \mu R(t), \; R(0) = R_0 \geq 0.
\end{aligned}
\tag{1}
$$

In this context, the proportions for the variables S, I, and R, are considered, with the constraint that $S + I + R = 1$. This mathematical framework has found applications in various fields. For instance, it has been adapted to model the propagation of computer viruses, as discussed in [20]. Additionally, the concept of the reproductive number, crucial to understanding the dynamics of disease transmission and control strategies, is explored in [18]. Furthermore, researchers have expanded the model by incorporating spatial diffusion to examine the influence of geographical factors on disease spread, as demonstrated in [9]. Most recently, in the context of the COVID-19 pandemic, the SIR model has been used to estimate the prevalence of infection by combining it with statistical methods, as detailed in [11].

One limitation of the SIR model is that once individuals have moved into the recovered class, they cannot transition back to either the susceptible or infected class. This limitation means that it

N. Susyanto

Malaysian J. Math. Sci. 19(1): 311–323(2025) *311 - 323*

cannot be applicable in certain contexts. For instance, in cases of influenza and COVID-19, recovered individuals can become susceptible again and subsequently become infected. This scenario has been explored in the context of modelling influenza in a study by Coburn et al. [3] and modelling COVID-19 in research conducted by Salman et al. [12], where both studies use a modified SIR model known as the SIRS model.

In some cases, individuals who have already moved into the recovered class can transition directly back into the infected class, especially when modelling addiction-related phenomena. The model is referred to as the ARSIRI (Addiction-Related SIR model). For example, due to the addictive nature of nicotine, individuals who have quit smoking can relapse and become smokers again, akin to being "reinfected". Here, the concept of "infection" refers to smoking behavior. The spread of smoking behavior has been examined in previous studies [13, 21]. However, these studies do not account for the possibility of reinfection. Another addiction-related phenomenon is alcohol use disorders. Our ARSIRI model has the potential to model alcohol use and abuse in rural areas, as highlighted in the study by Osgood and Chambers [10]. This represents the first contribution of our current paper.

From a broader perspective, this paper investigates the ARSIRI model, illustrated in Figure 2. This model serves as an extension of the existing SIR model, incorporating an additional reinfection parameter denoted as ω. The concept of modelling with reinfection was initially introduced in [17], primarily to model herpes infections. Although stability criteria were provided, the studies in this direction lacked an analysis of reproductive numbers and bifurcations. Subsequently, the SIRI model has been explored from various angles in other studies [14, 1]. However, despite the stability and bifurcation analyzes in these papers, none of them thoroughly investigate the reinfection parameter, which sets ARSIRI apart from the standard SIR model. Among all mentioned advantages, the proposed method should satisfy all assumptions like what the SIR model does, such as homogeneous mixing of the infected and susceptible populations and a constant total population over time.

The second major contribution of our current paper lies in conducting a comprehensive examination of the reinfection parameter. This involves assessing its impact on reproductive number and stability, as well as providing a bifurcation analysis. Furthermore, consequences of neglecting this reinfection parameter are explored, both through simulated data analysis and through real data analysis. The real data used in our study pertain to alcohol use disorders taken from Our World in Data. The remainder of the paper proceeds as follows. Section 2 presents the main results, including the ARSIRI mathematical model, reproductive numbers, the existence of equilibrium points, their stability, and an analysis of the effects of the reinfection parameter, including bifurcation analysis. To illustrate the performance of the ARSIRI model compared to the standard SIR model, both simulated and real datasets are utilized, considering the mean square errors of both models. Finally, Section 4 draws some conclusions.
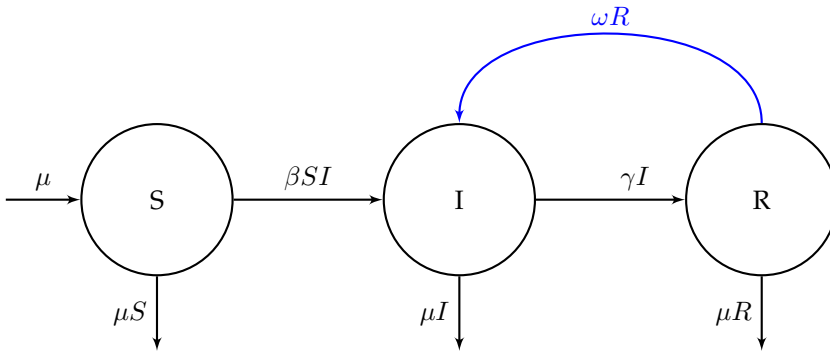
Figure 2: SIRI Diagram Transfer

2   Main Results

With the reinfection parameter ω, our ARSIRI model is a system of differential equations,

$$
\begin{aligned}
\frac{dS(t)}{dt} &= \mu - \beta S(t)I(t) - \mu S(t),\ S(0) = S_0 \geq 0,\\
\frac{dI(t)}{dt} &= \beta S(t)I(t) + \omega R(t) - \mu I(t) - \gamma I(t),\ I(0) = I_0 \geq 0,\\
\frac{dR(t)}{dt} &= \gamma I(t) - \omega R(t) - \mu R(t),\ R(0) = R_0 \geq 0,
\end{aligned}
\tag{2}
$$

with domain $\Omega = \{(x,y,z) \in \mathbb{R}^3 : x,y,z \geq 0 \text{ and } x+y+z = 1\}$. It is easy to see that Ω is positively invariant with respect system 2.

2.1   Reproductive number and stability of equilibrium points

The quantity threshold that can be used to determine whether infection can invade and persist in a new host population is called the reproductive number. Using the next-generation method (NGM) as provided in [19], the reproductive number of the model (1) can be easily obtained, which is equal to $R_0^{SIR} = \dfrac{\beta}{\mu + \gamma}$. Unfortunately, this method cannot be used for ARSIRI because the disease-free population is not invariant. Note that even though the population is free of disease, it is still possible for the population to get infection due to the reinfection rate ω. Therefore, another approach is needed to find this reproductive number.

In order to obtain the reproductive number, the Jacobian matrix at the equilibrium points is considered. Now, let us define,

$$
R_0 = \frac{\beta(\mu + \omega)}{\mu(\mu + \omega + \gamma)}.
\tag{3}
$$

Next, it will be proved that this R_0 satisfies two natural properties of the reproductive number:

- if it is less than 1, then the disease must be dying out and,

- if it is greater than 1, then the disease persists in the population.

The first property can be seen by the stability of the disease-free equilibrium point, whereas the second one can be seen from the endemic equilibrium point. The results are provided in the following theorems.

Theorem 2.1. *If $R_0 < 1$, the model* (2) *has a disease-free equilibrium point $E_0 = (1,0,0)$ that is locally asymptotically stable.*

Proof. It is clear that substituting E_0 into system (2) results in $\dfrac{dS}{dt} = 0$, $\dfrac{dI}{dt} = 0$, and $\dfrac{dI}{dt} = 0$. Note that the Jacobian matrix at E_0 is ,

$$Jf(E_0) = \begin{bmatrix} -\mu & -\beta & 0 \\ 0 & \beta - \mu - \gamma & \omega \\ 0 & \gamma & -\mu - \omega \end{bmatrix}. \tag{4}$$

The characteristic polynomial of $Jf(E_0)$, i.e.,

$$p_0(\lambda) = det(\lambda I - Jf(E_0)) = (\lambda + \mu)((\lambda - \beta + \mu + \gamma)(\lambda + \mu + \omega) - \omega\gamma), \tag{5}$$

has roots $\lambda_1 = -\mu < 0$ and zeros of the quadratic polynomial,

$$(\lambda + a)(\lambda + b) - c = 0, \tag{6}$$

with $a = -\beta + \mu + \gamma, b = \mu + \omega$, and $c = \omega\gamma$. To ensure that the roots of (6) have the negative real part, it is sufficient to show that $a + b$ and $ab - c$ are positive. These two conditions can be verified by using the fact that $R_0 < 1$ as follows,

$$a + b = -\beta + \mu + \gamma + \mu + \omega = -\beta + \frac{\beta(\mu + \omega)}{\mu R_0} + \mu > -\beta + \frac{\beta(\mu + \omega)}{\mu} + \mu > \mu > 0,$$

and

$$ab - c = (-\beta + \mu + \gamma)(\mu + \omega) - \omega\gamma = -\beta(\mu + \omega) + (\mu + \gamma)(\mu + \omega) - \omega\gamma,$$
$$= -R_0\mu(\mu + \omega + \gamma) + \mu^2 + (\omega + \gamma)\mu > -\mu(\mu + \omega + \gamma) + \mu^2 + (\omega + \gamma)\mu = 0.$$

This proves that E_0 is locally asymptotically stable, as required. □

Next, the property related to the stability of the endemic equilibrium point is investigated.

Theorem 2.2. *If $R_0 > 1$, the model* (2) *has a unique endemic equilibrium point $E_+ = (S^*, I^*, R^*)$ that is locally asymptotically stable where,*

$$S^* = \frac{1}{R_0}, \tag{7}$$

$$I^* = \frac{\mu(R_0 - 1)}{\beta}, \tag{8}$$

$$R^* = \frac{\gamma\mu(R_0 - 1)}{\beta(\mu + \omega)}. \tag{9}$$

Proof. By vanishing the right-hand side of each equation in (2),

$$0 = \mu - \beta S^* I^* - \mu S^* \iff S^* = \frac{\mu}{\beta I^* + \mu}, \tag{10}$$

$$0 = \beta S^* I^* - \mu I^* - \gamma I^* + \omega R^*, \tag{11}$$

$$0 = \gamma I^* - \omega R^* - \mu R^* \iff R^* = \frac{\gamma I^*}{\omega + \mu}, \tag{12}$$

N. Susyanto

Malaysian J. Math. Sci. 19(1): 311–323(2025) 311 - 323

is obtained. Plugging (10) and (12) into (11) gives $I^* = \dfrac{\mu(R_0 - 1)}{\beta}$ and subsequently $S^* = \dfrac{1}{R_0}$ and $R^* = \dfrac{\gamma\mu(R_0 - 1)}{\beta(\mu + \omega)}$ as claimed. Next, the stability of E_+ is investigated using a Jacobian matrix. The Jacobian matrix at E_+ is computed to be,

$$Jf(E_+) = \begin{bmatrix} -\beta I^* - \mu & -\beta S^* & 0 \\ \beta I^* & \beta S^* - \mu - \gamma & \omega \\ 0 & \gamma & -\omega - \mu \end{bmatrix}, \tag{13}$$

that has characteristics equation,

$$(\lambda + \mu)(\lambda - (\beta S^* - \beta I^* - \mu - \gamma))\left(\lambda + \frac{-\gamma(\omega - \beta I^*)}{\beta S^* - \beta I^* - \mu - \gamma} - (\omega + \mu)\right) = 0. \tag{14}$$

Consequently, the eigen values of (13) are,

$$\lambda_1 = -\mu,$$
$$\lambda_2 = \beta S^* - \beta I^* - \mu - \gamma,$$

and

$$\lambda_3 = \frac{-\gamma(\omega - \beta I^*)}{\beta S^* - \beta I^* - \mu - \gamma} - (\omega + \mu).$$

Since λ_1 is clearly negative, only the need to show $\lambda_2, \lambda_3 < 0$. The eigen value λ_2 can be written as,

$$\lambda_2 = -\frac{\gamma\omega}{\mu + \omega} - \mu(R_0 - 1),$$

that is clearly negative for $R_0 > 1$. The last eigen value λ_3 can be written as,

$$\lambda_3 = \frac{\mu(\mu + \omega + \gamma)(R_0 - 1)}{\lambda_2},$$

that is also obviously negative for $R_0 > 1$ since $\lambda_2 < 0$. □

2.2 The effects of reinfection parameter

The reinfection parameter ω plays a crucial role in the SIRI model by increasing the basic reproductive number compared to the standard SIR model. This fact can be verified by the relation between R_0 and R_0^{SIR}, that is,

$$R_0 = \left(1 + \frac{\gamma\omega}{\mu(\mu + \omega + \gamma)}\right) R_0^{SIR}. \tag{15}$$

Consequently, it follows that if an SIR model possesses a reproductive number greater than one, then its corresponding SIRI model (with identical parameters to the SIR model except for the reinfection parameter) will also have a reproductive number greater than one.

Note that the reproductive number R_0 is an increasing function of ω, *cateris paribus*. What makes this intriguing is that while the SIR model may have a reproductive number less than one

(indicating the disease dies out), the corresponding SIRI model can have a reproductive number greater than one if the reinfection rate is sufficiently high, as illustrated in Figure 3. It becomes evident that when starting with $R_0 < 1$, there exists a specific value of ω such that $R_0 > 1$. The value of ω^* at which R_0 equals one serves as the bifurcation parameter.
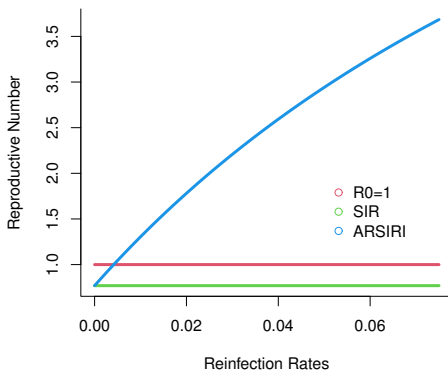

Figure 3: Comparison of reproductive numbers.

For each value of R_0, the corresponding ω, as determined by (3), is given by the equation:

$$\omega = \frac{\mu([\mu + \gamma]R_0 - \beta)}{\beta - \mu R_0}.$$ (16)

Consequently, the specific ω^* corresponding to $R_0 = 1$ is:

$$\omega^* = \frac{\mu(\mu + \gamma - \beta)}{\beta - \mu}.$$ (17)

It is important to note that the graph of R_0 as a function of ω intersects the line $R_0 = 1$ only when $\mu + \gamma > \beta$. This condition implies that if $\beta > \mu$ and $\mu + \gamma > \beta$, then the positive value for ω^* exists, leading to the emergence of a bifurcation as provided in the following theorem.

Theorem 2.3. *If $\beta > \mu$ and $\mu + \gamma > \beta$, then the bifurcation of system (2) at $\omega = \omega^*$ is forward.*

Proof. By employing the Castillo-Song bifurcation analysis [2], it is shown that the system (2) exhibits a forward bifurcation when $R_0 = 1$. Given that this value of $R_0 = 1$ corresponds to $\omega = \omega^*$ and considering that R_0 strictly increases with ω, it can be concluded that system (2) experiences a forward bifurcation at $\omega = \omega^*$. The graph illustrates that when $\omega < \omega^*$, there exists a unique stable equilibrium point, namely, the disease-free state. Conversely, when $\omega > \omega^*$, two equilibrium points emerge: one representing the unstable disease-free state and the other representing the stable endemic equilibrium point. □

An illustration of the forward bifurcation at $\omega = \omega^*$ is provided in Figure 4. The graph illustrates that when $\omega < \omega^*$, there exists a unique stable equilibrium point, namely, the disease-free state. Conversely, when $\omega > \omega^*$, two equilibrium points emerge: one representing the unstable disease-free state and the other representing the stable endemic equilibrium point.
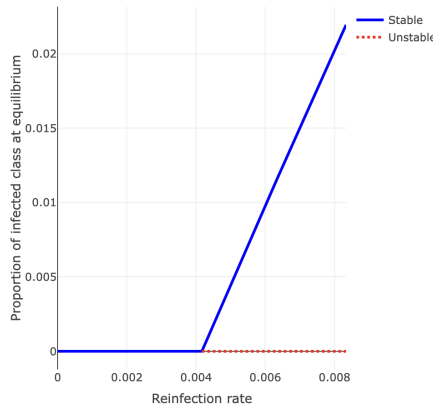
Figure 4: Bifurcation w.r.t. reinfection parameter.

3   Experimental Results

In this section, we apply the ARSIRI model to both simulated and real data on alcohol addiction. Parameter estimation for the SIR and SIRI models is obtained via ordinary least squares.

3.1   Simulated data

In the first simulated dataset, parameters $\beta = 0.12, \gamma = 0.1, \mu = 0.05$, and $\omega = 0.09$ are selected to simulate a scenario where $R_0 < 1$. With initial values $I(0) = 0.03$ and $R(0) = 0.05$, the values of $I(1), I(2), \ldots, I(15)$ are computed. The values of $R(1), R(2), \ldots, R(15)$ are not computed since these values are typically not reported in reality. Based on the computed values of $I(1), I(2), \ldots, I(15)$, the parameters $\beta, \gamma, \mu, \omega$, and the initial value $R(0)$ are estimated using a simple least squares method. Once the parameters are obtained, the mean square error (MSE) between the simulated data and the values predicted by the model is calculated.

To facilitate a comparison with the regular SIR model, the simulated data is also fitted with the standard SIR model and computed the MSE. The comparison between the ARSIRI and SIR models in the first simulated dataset is presented in Figure 5. Visually, it is evident that the SIRI model provides a much better fit compared to its counterpart, the SIR model. Numerically, the mean square errors (MSE) for the SIRI and SIR models have been verified as 0.04% and 0.30%, respectively.

This example illustrates that when the SIR model is applied to an SIRI case, the conclusion is incorrect. Note that $R_0^{SIR} = 0.8 < 1$ while $R_0 = 1.4 > 1$ so the SIR model will predict that the "disease" will die out, but the SIRI model will indicate that the endemic equilibrium is stable. From a bifurcation point of view, as provided by Theorem 2.3, the value of the reinfection parameter $\omega = 0.05$ is sufficient to change the stability of the endemic equilibrium point, since the critical point for this reinfection parameter is $\omega^* = 0.02142857$.

N. Susyanto

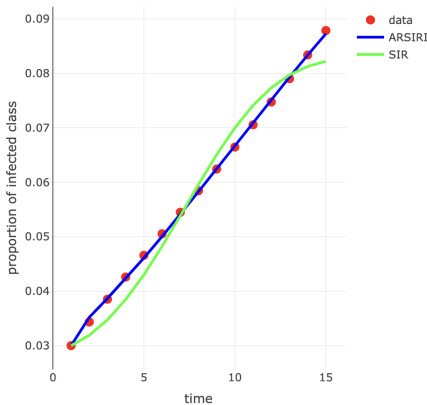*Malaysian J. Math. Sci. 19*(1): 311–323(2025) *311 - 323*

Figure 5: ARSIRI vs SIR in simulated data 1.

The second simulated dataset is designed to simulate a scenario where $R_0 > 1$. The same initial values and procedures are used as before, but parameters $\beta = 3, \gamma = 2.9, \mu = 0.0125$, and $\omega = 0.8$ are selected. The results are presented in the Figure 6, and the mean square errors (MSE) for the SIRI and SIR models are 3.74×10^{-5} and 6.7×10^{-3} respectively. This indicates that the ARSIRI model outperforms the SIR model.
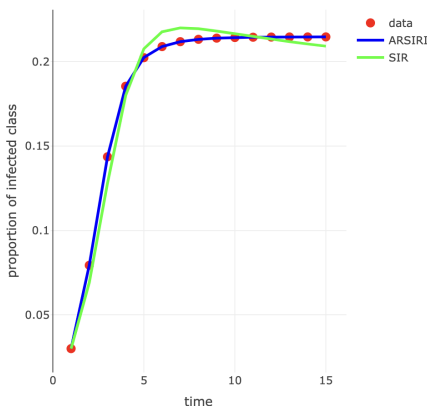

Figure 6: ARSIRI vs SIR in simulated data 2.

With $R_0^{SIR} = 1.030043 > 1$, the value of the reinfection rate $\omega = 0.8$ will dramatically increase $R_0 = 52.53$, which is approximately 50 times the reproductive number under the SIR model.

3.2 Real data

The ARSIRI model is applied to real data related to alcohol addiction, obtained from Our World in Data, specifically data on the current number of cases of alcohol use disorders per 100 people aged 15-49 years.This age group is selected because they are still actively interacting with others, making it relevant to the ARSIRI and SIR models.

The data spans from 1990 to 2019 for many countries, but The United Kingdom (UK) and

the United States are specifically selected due to their low birth rates. However, to adhere to the constant population condition required by our model, data only from 2013 to 2019 is used. Years prior to 2013 are excluded to ensure that the total population difference from 2019 remains below 5%.

Using these seven values of I, representing people with alcohol problems from both countries, the parameters $\beta, \gamma, \mu, \omega$, and the initial value $R(0)$ are estimated for our ARSIRI model. The parameters β, γ, μ, and ω are also estimated for the standard SIR model. Similar to the simulated data analysis, the mean square errors (MSEs) for both models are then compared.

The results in terms of graphics can be seen in Figure 7 for the United States, where the mean square error (MSE) for the ARSIRI model is 6.31×10^{-5}, outperforming the SIR model with an MSE of 9.24×10^{-5}.
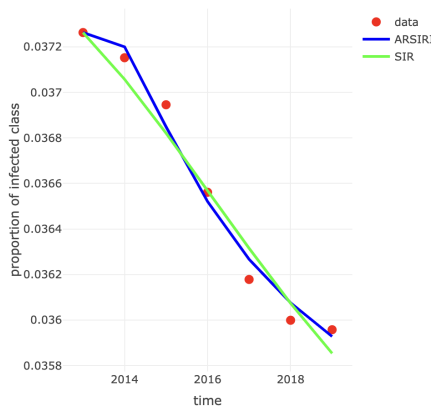

Figure 7: ARSIRI vs SIR for USA data.

For the UK, the results are presented in Figure 8, showing an MSE of 1.15×10^{-4} for our ARSIRI model and an MSE of 1.63×10^{-4} for the SIR model. It is evident that the ARSIRI model still slightly outperforms the SIR model in terms of MSE.
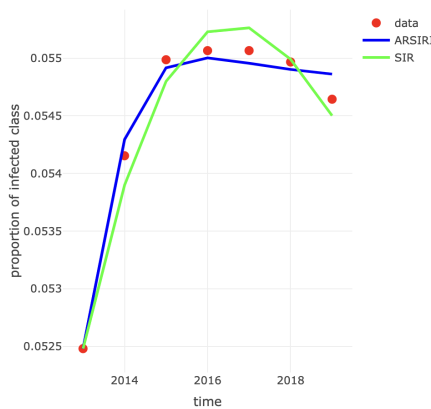

Figure 8: ARSIRI vs SIR for UK data.

It can be observed from the two real datasets above that when the SIR model is employed to model SIRI phenomena, the conclusions may be inaccurate, as depicted in Figures 7 and 8. These disparities could arise from the omission of reinfection when utilizing the SIR model for

modelling.

4   Conclusions

The ARSIRI model is explored, which represents addiction-related phenomena. After analyzing the existence of equilibrium points and their stability, the reproductive number is calculated using a straightforward Jacobian approach, even though it cannot be determined using the standard next-generation matrix approach. A simple analytical proof is also provided to justify the occurrence of forward bifurcation related to the reinfection parameter and its connection to the reproductive number. Using both simulated and real data, it is demonstrated that the ARSIRI model outperforms the standard SIR model.

The next research may focus on systems where the population is not constant. Furthermore, a stochastic version of the ARSIRI model might be of interest to consider, as it allows for different effects of infection and reinfection rates on different individuals. Lastly, exploring and validating applications related to addiction phenomena with real data could also be fruitful avenues for research.

Conflicts of Interest The authors declare no conflict of interest.

References

[1] A. Bernoussi, K. Hattaf et al. (2021). Global dynamics of an SIRSI epidemic model with discrete delay and general incidence rate. *Journal of Applied Nonlinear Dynamics*, 10(3), 547–562. https://doi.org/10.5890/JAND.2021.09.013.

[2] C. Castillo Chavez & B. Song (2004). Dynamical models of tuberculosis and their applications. *Mathematical Biosciences & Engineering*, 1(2), 361–404. https://doi.org/10.3934/mbe.2004.1.361.

[3] B. J. Coburn, B. G. Wagner & S. Blower (2009). Modeling influenza epidemics and pandemics: insights into the future of swine flu (H1N1). *BMC medicine*, 7, 1–8. https://doi.org/10.1186/1741-7015-7-30.

[4] M. M. Helal, R. M. Yaseen, A. A. Mohsen, H. F. AL Husseiny & Y. Sabbar (2024). Dynamics of a social model for marriage and divorce relationship with fear effect. *Malaysian Journal of Mathematical Sciences*, 18(2), 267–286. https://doi.org/10.47836/mjms.18.2.04.

[5] M. M. M. Ihsanjaya & N. Susyanto (2019). Mathematical model of changes in smoking behavior which involves smokers who temporarily and permanently quit smoking. In *Proceedings of the 8th SEAMS-UGM International Conferences on Mathematics and Its Applications 2019: Deepening Mathematical Concepts for Wider Application through Multidisciplinary Research and Industries Collaborations*, volume 2192 pp. Article ID: 060011. AIP Publishing, Yogyakarta, Indonesia. https://doi.org/10.1063/1.5139157.

[6] W. O. Kermack & A. G. McKendrick (1927). A contribution to the mathematical theory of epidemics. In *Proceedings of the royal society of london. Series A, Containing papers of a mathe-*

N. Susyanto

Malaysian J. Math. Sci. 19(1): 311–323(2025) *311 - 323*

matical and physical character, volume 115 pp. 700–721. The Royal Society London, London. https://doi.org/10.1098/rspa.1927.0118.

[7] S. Khajanchi, S. Bera & T. K. Roy (2021). Mathematical analysis of the global dynamics of a HTLV-I infection model, considering the role of cytotoxic T-lymphocytes. *Mathematics and Computers in Simulation*, *180*, 354–378. https://doi.org/10.1016/j.matcom.2020.09.009.

[8] G. S. Kumar & C. Gunasundari (2023). Dynamical analysis of two-preys and one predator interaction model with an Allee effect on predator. *Malaysian Journal of Mathematical Sciences*, *17*(3), 263–281. https://doi.org/10.47836/mjms.17.3.03.

[9] S. L. Li, J. P. Messina, O. G. Pybus, M. U. G. Kraemer & L. Gardner (2021). A review of models applied to the geographic spread of Zika virus. *Transactions of The Royal Society of Tropical Medicine and Hygiene*, *115*(9), 956–964. https://doi.org/10.1093/trstmh/trab009.

[10] D. W. Osgood & J. M. Chambers (2000). Social disorganization outside the metropolis: An analysis of rural youth violence. *Criminology*, *38*(1), 81–116. https://doi.org/10.1111/j.1745-9125.2000.tb00884.x.

[11] H. Salje, C. Tran Kiem, N. Lefrancq, N. Courtejoie, P. Bosetti, J. Paireau, A. Andronico, N. Hozé, J. Richet, C. L. Dubost et al. (2020). Estimating the burden of SARS-CoV-2 in France. *Science*, *369*(6500), 208–211. https://doi.org/10.1126/science.abc3517.

[12] A. M. Salman, I. Ahmed, M. H. Mohd, M. S. Jamiluddin & M. A. Dheyab (2021). Scenario analysis of COVID-19 transmission dynamics in malaysia with the possibility of reinfection and limited medical resources scenarios. *Computers in Biology and Medicine*, *133*, Article ID: 104372. https://doi.org/10.1016/j.amc.2007.09.053.

[13] B. T. G. Shweta Bansal & L. A. Meyers (2007). When individual behaviour matters: homogeneous and network models in epidemiology. *Journal of The Royal Society Interface*, *4*(16), 879–891. https://doi.org/10.1098/rsif.2007.1100.

[14] S. Side, M. I. Pratama, N. Badwi & W. Sanusi (2020). Analysis and simulation of SIRI model for dengue fever transmission. *Indian Journal of Science and Technology*, *13*(3), 340–351. https://doi.org/10.17485/ijst/2020/v13i03/147852.

[15] N. Susyanto, R. Veldhuis, L. Spreeuwers & C. Klaassen (2019). Semiparametric likelihood-ratio-based biometric score-level fusion via parametric copula. *IET biometrics*, *8*(4), 277–283. https://doi.org/10.1049/iet-bmt.2018.5106.

[16] P. K. Tiwari, R. K. Rai, S. Khajanchi, R. K. Gupta & A. K. Misra (2021). Dynamics of coronavirus pandemic: effects of community awareness and global information campaigns. *The European Physical Journal Plus*, *136*(10), Article ID: 994. https://doi.org/10.1140/epjp/s13360-021-01997-6.

[17] D. Tudor (1990). A deterministic model for herpes infections in human and animal populations. *Siam Review*, *32*(1), 136–139. https://doi.org/10.1137/1032003.

[18] P. Van den Driessche (2017). Reproduction numbers of infectious disease models. *Infectious Disease Modelling*, *2*(3), 288–303. https://doi.org/10.1016/j.idm.2017.06.002.

[19] P. Van den Driessche & J. Watmough (2002). Reproduction numbers and sub-threshold endemic equilibria for compartmental models of disease transmission. *Mathematical Biosciences*, *180*(1-2), 29–48. https://doi.org/10.1016/S0025-5564(02)00108-6.

[20] L. X. Yang & X. Yang (2014). A new epidemic model of computer viruses. *Communications in Nonlinear Science and Numerical Simulation*, *19*(6), 1935–1944. https://doi.org/10.1016/j.cnsns.2013.09.038.

N. Susyanto

Malaysian J. Math. Sci. 19(1): 311–323(2025) 311 - 323

[21] G. Zaman, Y. H. Kang, G. Cho & I. H. Jung (2017). Optimal strategy of vaccination & treatment in an SIR epidemic model. *Mathematics and Computers in Simulation*, *136*, 63–77. https://doi.org/10.1016/j.matcom.2016.11.010.

[22] F. Zhang, Z. Z. Li & F. Zhang (2008). Global stability of an SIR epidemic model with constant infectious period. *Applied Mathematics and Computation*, *199*(1), 285–291. https://doi.org/10.1016/j.amc.2007.09.053.